Cement and Concrete Research 132 (2020) 106066

Contents lists available at ScienceDirect

Cement and Concrete Research

journal homepage: www.elsevier.com/locate/cemconres

Short communication

Synchrotron X-ray Raman scattering shows the changes of the Ca environment in C-S-H exposed to high pressure

Jiaqi Li*, Wenxin Zhang, Paulo J.M. Monteiro

Department of Civil and Environmental Engineering, University of California, Berkeley, CA 94720, United States

ARTICLE INFO

Keywords:
Calcium silicate hydrate
High-pressure
X-ray Raman
Deformation
Coordination

ABSTRACT

X-ray Raman Scattering (XRS) is a new probe to analyze the local chemical environment of elements of interest. In this communication, XRS is, for the first time, used in the field of cement study. In situ high-pressure XRS (HP-XRS) at Ca $L_{2,3}$-edge was used to examine the pressure-induced change of Ca environment of C-S-H under a loading/unloading cycle of combined deviatoric stress and hydrostatic pressure up to 20 GPa. The peak positions of the Ca $L_{2,3}$-edge systematically shifted to lower energies upon loading, suggesting a shortening of the Ca—O bonds. The peak positions of the Ca $L_{2,3}$-edge shifted to higher energies upon unloading, but permanent shifts in edge positions were observed after unloading to 0 GPa, suggesting a permanent deformation mainly due to a distortion in the interlayer Ca and a sliding at interlayer region. For the first time, the pressure-induced structural change of C-S-H is evidenced at the atomic scale.

1. Introduction

Calcium silicate hydrate (C-S-H), the primary binding phase in concrete, controls the mechanical and has a significant importance in the durability of concrete [1]. C-S-H has a layered structure analogous to defective tobermorite (a CaO_7 sheet sandwiched by silicate tetrahedra chains and hydrous interlayers) [2] with variable chemical compositions [3]. This silicate chain consists of polymerized tetrahedral units – one bridging tetrahedron and two paired tetrahedra. The bridging site is replaced by interlayer Ca when Ca/Si ratio increases [4]. Synthetic C-S-H (also termed C-S-H(I)) has a poorly ordered layer-stacking, and the stacking is even poorer for C-S-H in hardened cement [5]. The size of C-S-H representative domains has been estimated to be ~5 nm [6,7].

Understanding the mechanical properties of C-S-H at phase-pure level can advance the optimization of concrete using a bottom-up approach. In nanoindentation studies, when indentation depth is below 500 nm [8], the contribution of portlandite on indentation modulus of C-S-H can usually be eliminated [9]. However, nanoindentation only probes the mechanical properties of C-S-H at a high hierarchical level – where the C-S-H building blocks interconnect with water/gas/epoxy-filled nanometer-size gel pores [10]. In addition, the sample preparation for nanoindentation requires an extremely flat surface, the polishing process of sample surfaces may slightly alter the results. The influences of pores at nano [11] to even macro [12] scales on the measurement of mechanical properties of C-S-H cannot be omitted in studies at different hierarchical levels.

The mechanical properties of pure C-S-H have been investigated using atomistic modelling [13,14]. The theoretical calculations have been experimentally validated down to the unit-cell scale using high-pressure X-ray diffraction (HP-XRD) [15,16], which eliminates the influence of nanopores between C-S-H nano-domains. However, determining the pressure-induced structural change at atomic scale from HP-XRD refinement is challenging due to the poorly-crystalline nature of C-S-H [17] and the typical amorphization of cement hydration products under high pressure [18]. The ordering of layer-stacking of C-S-H is typically poor at low Ca/Si ratio or with Al incorporation at room temperature [19]. Our recent in situ study using high-pressure Raman spectroscopy, a commonly used technique in geological studies, showed that the interatomic interaction in silicate tetrahedra of C-S-H under pressure can be probed [20]. However, the Ca—O signal under the pressure was not intense enough to be measured reliably. Another technique for probing local bonding nature is X-ray absorption spectroscopy (XAS) [21]. Unfortunately, for a high-pressure diamond anvil cell (DAC), the transmission of hard X-ray through a gasket and diamond anvils typically requires energy above 6 keV, which exceeds the K-edge (i.e., 4050 eV) of Ca- the heaviest element in C-S-H [22,23].

X-ray Raman scattering (XRS, also known as non-resonant synchrotron inelastic X-ray scattering) spectroscopy is a new probe for the determination of the element-specific local bonding environment. In

* Corresponding author.
E-mail address: jiaqi.li@berkeley.edu (J. Li).

https://doi.org/10.1016/j.cemconres.2020.106066
Received 6 February 2020; Received in revised form 24 March 2020; Accepted 28 March 2020
Available online 10 April 2020

this synchrotron-based technique, electronic transitions at soft X-ray absorption edges are excited using hard X-ray, typically ~ 10 keV, by tuning the energy loss between incident and scattered X-ray energy [22]. XRS is ideal to obtain chemical information of light elements with bulk-sensitivity [24]. The energy loss in XRS typically ranges from ~0 eV to 1100 eV, which covers Si L-edge, Ca $L_{2,3}$-edge, and O K-edge. Thus, the in-situ pressure-induced change in exciton energy of elements of interest in C-S-H can only be measured in a DAC using high-pressure X-ray Raman scattering (HP-XRS) spectroscopy.

In this study, we probe the in-situ pressure-induced change in calcium environment of C-S-H using HP-XRS spectroscopy at Ca $L_{2,3}$-edge. The influence of gel pores, even at the nanoscale, is eliminated. A loading/unloading cycle of combined deviatoric stress with hydrostatic pressure is applied to the pure C-S-H sample. For the first time, the pressure-induced structural change of Ca in C-S-H is evidenced. Our results exhibit a great potential in the use of this emerging technique in cement-related studies. The use of HP-XRS is not limited by the crystallinity and amorphization of samples or certain impurities. The application and limitation of this technique in cement studies are discussed.

2. Materials and experiment

C-S-H was synthesized at an initial bulk Ca/Si molar ratio of 1.4, by mixing CaO and SiO_2 at a water-to-solid mass ratio of 45 in a N_2-filled glove box, and cured at 20 °C for 182 days. The solid was vacuum filtered using 450-nm nylon filters, freeze-dried for 7 days, and then stored in N_2-filled desiccators at 30% relative humidity. The final Ca/Si ratio was measured to be 1.29 [19].

HP-XRS experiment was performed at ~25 °C using a panoramic DAC at beamline 16-IDD of the High Pressure Collaborative Access Team (HPCAT) at the Advanced Photon Source (APS) in the Argonne National Laboratory. The undulator beamline provides monochromatic X-rays at ~10.2 keV with beam size of 3 μm × 5 μm. Three columns of 50.8-mm diameter bent Si (111) analyzers (fixed energy at 9.903 keV) were mounted on an 870-mm vertical Rowland circle to refocus inelastically scattered X-ray photons onto a Si detector at a scattering angle of 30° to the focusing poly-capillary in a backscattering geometry. The incident beam is perpendicular to the principal loading direction. The averaged momentum transfer (q) in this study is 2.65 $Å^{-1}$. The energy resolution of this beamline setup is 1.0 eV. For more details of the beamline setup, see [25]. This beamline setup with a focusing poly-capillary is optimized for signal/noise ratio with certain compromise of scattering angle (a fixed scattering angle), resulting in an intermediate level of q. Otherwise, the data collection time can be five times longer. Given the beamline setup, the collection time of a single dataset at Ca $L_{2,3}$-edge was 8–12 h with an average of 11 h.

A Be gasket (Easymaterials, China) was pre-indented by diamond anvils (400-μm culet diameter) to a thickness of ~50 μm, and then a ~90-μm diameter cylindrical chamber was laser-drilled at the gasket center. The drilled gasket was carefully rinsed with reagent-grade ethanol in a fume hood. The powder sample, with a ruby sphere (as a pressure gauge), was loosely loaded into the chamber. A thin layer of polyimide foil was wrapped around the backseats in the DAC to isolate any potential Be/BeO dust if the experiment fails and the Be gasket explodes. Pressure transmitting medium was not used in this HP-XRS study; therefore, a deviatoric stress is generated (~10% of the pressure indicated by ruby) [28]. Note that, in previous HP-XRD studies of cement-related samples, pressure medium (e.g., methanol/ethanol mixed solution or silicone oil [26,27]) was used to provide a hydrostatic pressure in the gasket chamber. However, pressure medium is not often used in the HP-XRS study for minimizing scattering and/or absorption from the pressure medium [22]. Moreover, these pressure media would provide inevitable artifacts during the collection of O K-edge and/or Si L-edge XRS spectra, if applicable in any further data collection. For the ambient-pressure XRS measurement, the dry powder was loaded into a thin-walled polyimide tube (400-μm diameter) and measured in a N_2-protected environment. The DAC was systematically loaded from ambient pressure to 20 GPa, then unloaded back to 0 GPa. After each pressure change, 15 min was waited for pressure stabilization before each HP-XRS measurement.

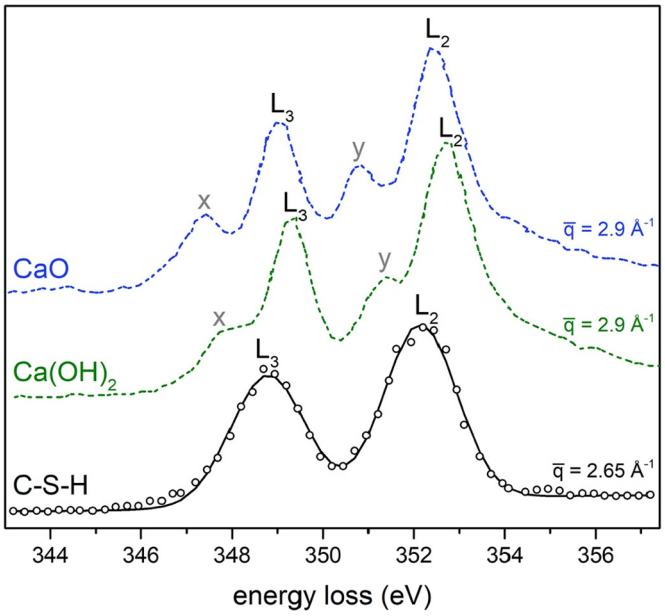

Fig. 1. Calcium $L_{2,3}$-edge XRS spectra of C-S-H, CaO, and portlandite. The XRS spectra of CaO and portlandite are from [28], and the energy calibration was unknown. The energy resolution in the present study is 1.0 eV (worse than 0.9 eV in [28]), also making the spectral comparison here meaningless.

3. Results and discussion

Fig. 1 shows the Ca $L_{2,3}$-edge of C-S-H, CaO [28], and portlandite [28]. The L_3 and L_2 peaks correspond to electronic exciton from 2p-state with total angular momentum of 3/2 and 1/2 to unoccupied states, respectively [22]. The XRS spectrum at the C-S-H Ca $L_{2,3}$-edge does not clearly exhibit two spin-orbital related weak pre-edge peaks (x and y) which are commonly observed in XAS spectrum of C-S-H [29,30]. These pre-edge peaks are sensitive to momentum transfer (i.e., q dependent) in XRS and are often more intense at higher momentum transfer [22,31]. However, the beamline setup here allows only an averaged q of 2.65 $Å^{-1}$ at Ca $L_{2,3}$-edge due to a fixed scattering angle at 30°, which likely precluded us from observing the pre-edge peaks. Measurement with a higher q at other beamlines (e.g., 20-ID at the European Synchrotron Radiation Facility (ESRF)) may reveal the pre-edge peaks in XRS [32]. Note that, a comparison of peak positions between the three phases here is meaningless as the energy calibration was unknown and the momentum transfer was different.

Fig. 2a shows the XRS spectra of C-S-H at different pressures. The peak positions of L_3 and L_2 peaks as a function of pressure are shown in Fig. 2b. The peak positions systematically decreased with an increased pressure, suggesting a lowered energy of unoccupied states of Ca. The same relation between pressure and energies of L_3 and L_2 was also observed in a HP-XRS study of $CaSiO_3$ glass [22]. The pressure-induced lower exciton energy corresponds to shorter Ca—O pair distance in C-S-H. Our previous simulation results showed that Ca—O pair distance of C-S-H shortens under hydrostatic pressure. After reaching 20 GPa, the DAC started to unload, and the exciton energy increased. The increased energy suggests a recovery from shortened Ca—O pairs. Interestingly, the shift of peak positions between ambient and unloaded 0 GPa shows that the change in exciton energy is not fully reversible. The energy shift suggests a relaxation of atomic position which results in a

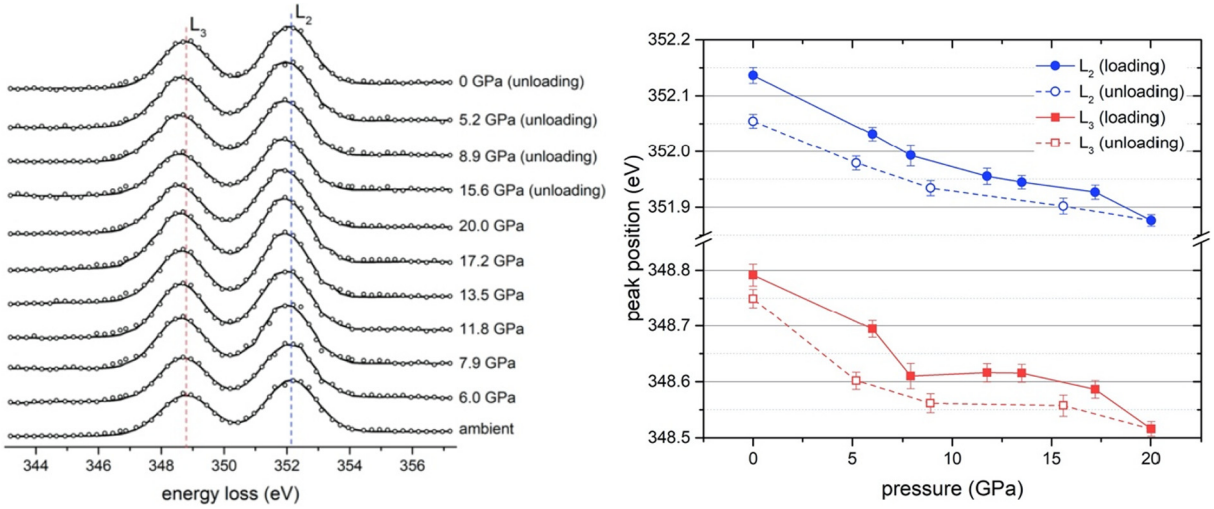

Fig. 2. a) Ca $L_{2,3}$-edge XRS spectra for C-S-H at varying pressures. After 20 GPa, the DAC was unloaded to 0 GPa. b) Peak positions of L_3 and L_2 in a). The data were fitted with Gaussian distribution.

permanent deformation (i.e., shortening) of Ca−O pair distance after unloading. A permanent deformation of −1.5% along the c-axis of a cross-linked Al-incorporated C-S-H (C-A-S-H) was found in our previous study using HP-XRD under a deviatoric stress [14,33].

We assign this Ca−O deformation mainly to the distortion of interlayer Ca and a sliding of interlayer. Richardson's T2_ac dimeric tobermorite-based model [4] with Ca/Si of 1.3 (see Fig. 3) can elucidate the Ca−O pairs. Although the average Ca−O bond length in six-fold coordination is typically shorter than that in seven-fold coordination, in this case 2.43 Å in six-fold coordination vs. 2.475 Å seven-fold coordination, the six-fold coordinated interlayer Ca connects to two water molecules (Ow). These two Ca-Ow bonds both have lengths of 2.69 Å while the bond lengths of other four Ca−O range from 2.28 to 2.32 Å. The Ca-O in CaO_7 sheet is the least deformable since the intralayer is much denser than the interlayer. Computational modelling is expected to provide additional insight into the pressure-induced atomistic change.

Trends in area or intensity ratio of the two peaks with applied pressure were not observed. The lack of such trends suggests the absence of a spin transition between L_3 and L_2 under pressure. The pressure up to 20 GPa is not high enough to force the transition of core electrons in Ca. Certainly the extreme stress condition of this sample in the DAC significantly exceeds the ultimate strength of even ultra high performance concrete under service [34]. Whereas, the applied compression on C-S-H samples or cement pastes by a nano-indenter can be a few GPa [35], and the shear stress can be even higher near the contact edge of the indenter due to stress concentration [36,37]. Such high stress may result in a permanent deformation of Ca−O in C-S-H. Thus, chemical analysis (e.g., optical Raman and infrared spectroscopy) around the nano-indents of C-S-H should be avoided.

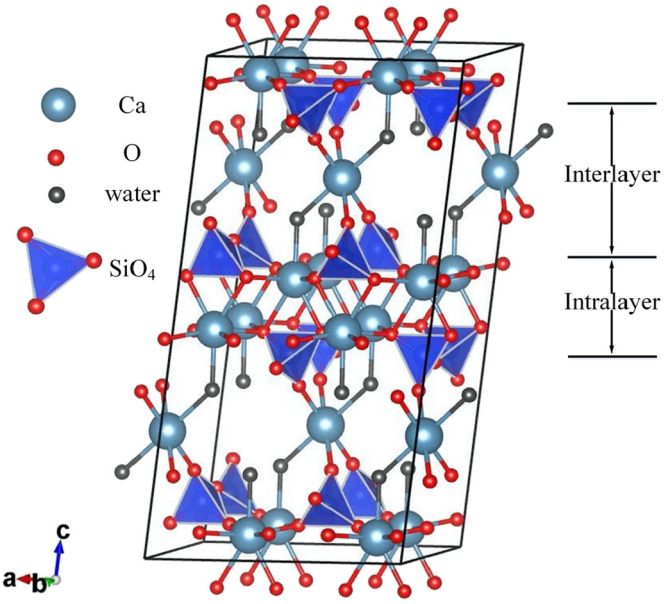

Fig. 3. The molecular structure of C-S-H (Ca/Si = 1.3) [4].

The present study shows a great potential in the use of HP-XRS in cement research. In addition to aforementioned advantages at Ca $L_{2,3}$-edge. For future studies and systematic comparisons in XRS spectra at Ca $L_{2,3}$-edge, a comprehensive dataset of CaO, portlandite, C-S-H, and C-S-H minerals (e.g., tobermorite and jennite), ideally measured at the same high level of q, is needed. HP-XRS also can be used to probe the pressure-induced change in environments of Si−O in C-S-H and C-A-S-H, from both synthetic phase-pure C-S-H samples and hydration of cement without concerning the crystallinity of C-S-H and any Ca-bearing impurities. Note that the optical Raman bands at wavenumber of 800–1000 cm^{-1} in hydration product C-S-H is very broad [38]; thus, the study of pressure-induced change in its Si-O(−Si) bond(s) is challenging when conventional optical Raman spectroscopy is used.

Future studies using HP-XRS are needed to explore the influence of mean silicate chain length, cross-linking of chains, and aluminum incorporation on pressure-induced change in Ca environment of C-S-H. Future experiments with pure hydrostatic conditions (with pressure-transmitting medium) are needed to understand the influence of stress conditions (hydrostatic versus non-hydrostatic) on the pressure-induced change in environment of Ca, O, and Si of C-S-H and other cement-related phases.

The limitations of HP-XRS application in cement-related study should not be ignored. The XRS data collection is inefficient since XRS inevitably excites inelastically scattered X-ray photons, the intensity of which is significantly lower than that of an elastic X-ray signal [22]. Thus, the current minimum collection time is 8–12 h for C-S-H at Ca $L_{2,3}$-edge at each pressure point. Typically, the required collection time for O K-edge and Si L-edge spectra can be even longer. A set of Ca $L_{2,3}$-edge as a function of pressure currently requires collection time of a few days. The current collection time under hydrostatic conditions, with the use of methanol/ethanol solution or silicone oil as the pressure medium, can be further elongated because the scattering and absorption of medium lowers the intensity of inelastically scattered X-ray (the attenuation is not negligible at ~10 KeV). The use of helium as a

pressure medium, although not commonly used in HP-XRS studies [32], can significantly lower the attenuation at energy of ~10 KeV. This DAC and gas loading setup will be considered in future studies. Fortunately, the fourth-generation synchrotron sources (e.g., upgraded ESRF and APS) [39], which are available soon, can be more than two orders of magnitude brighter than the current status of APS. Thus, the future collection time of HP-XRS at each pressure point is expected to be significantly reduced. Because XRS probes elements of interest, studies of C-S-H intermixes with portlandite or anhydrous silicate are challenging at Ca $L_{2,3}$-edge and/or Si L-edge.

The limitations of HP-XRS for general application are also notable. Beryllium is highly toxic when exposed to skin or by inhalation. After unloading of a DAC, the sample is often tightly embedded in a Be gasket. The extraction of an unloaded sample from the deformed Be gasket is challenging and hazardous. Further characterization of an unloaded sample without Be contaminant is very difficult.

4. Conclusions

In this communication, the use of HP-XRS to investigate the atomistic scale change of C-S-H has revealed new insight into the deformation of C-S-H under loading. For the first time, a permanent deformation of Ca—O in C-S-H has been evidenced after a full load-recovery. Hence, this new synchrotron-based technique is a valuable tool for investigating the atomistic change of semi-crystalline and even amorphous phases in cement-related studies.

CRediT authorship contribution statement

Jiaqi Li:Conceptualization, Methodology, Investigation, Writing - original draft.**Wenxin Zhang**:Investigation, Visualization, Writing - review & editing.**Paulo J.M. Monteiro**:Writing - review & editing, Supervision, Funding acquisition.

Declaration of competing interest

The authors declare that they have no known competing financial interests or personal relationships that could have appeared to influence the work reported in this paper.

Acknowledgement

We greatly honor Prof. James Kirkpatrick, deceased, who pioneered the NMR and Raman studies of C-S-H and other cement phases. We thank Barbara Lothenbach for providing the sample synthesized by Emilie L'Hôpital at the Laboratory for Concrete & Construction Chemistry (EMPA). Paul Chow at HPCAT is thanked for technical supports. The SusChEM program, Grant No. DMR-1410557, and the Division of Materials Research Ceramics Program, DMR-CER, Grant No. 1935604 of National Science Foundation are gratefully acknowledged. HPCAT experiments are supported by DOE-NNSA's Office of Experimental Sciences. The Advanced Photon Source is a U.S. Department of Energy (DOE) Office of Science User Facility operated for the DOE Office of Science by Argonne National Laboratory under Contract No. DE-AC02-06CH11357.

References

[1] P.K. Mehta, P.J. Monteiro, Concrete Microstructure, Properties and Materials, (2017).
[2] S. Merlino, E. Bonaccorsi, A.R. Kampf, Tobermorite 14 angstrom: crystal structure and OD character, Applied Mineralogy, vols 1 and 2, 2000, pp. 859–861.
[3] I.G. Richardson, The nature of C-S-H in hardened cements, Cem. Concr. Res. 29 (8) (1999) 1131–1147.
[4] I.G. Richardson, Model structures for C-(A)-S-H(I), Acta Crystallograph. Sect. B Struct. Sci. Cryst. Eng. Mater. 70 (2014) 903–923.
[5] H.F. Taylor, Cement Chemistry, 475 Academic press London, 1990.
[6] L.B. Skinner, S.R. Chae, C.J. Benmore, H.R. Wenk, P.J.M. Monteiro, Nanostructure of calcium silicate hydrates in cements, Phys. Rev. Lett. 104 (19) (2010).
[7] A.J. Allen, J.J. Thomas, H.M. Jennings, Composition and density of nanoscale calcium-silicate-hydrate in cement, Nat. Mater. 6 (4) (2007) 311–316.
[8] F.J. Ulm, M. Vandamme, H.M. Jennings, J. Vanzo, M. Bentivegna, K.J. Krakowiak, G. Constantinides, C.P. Bobko, K.J. Van Vliet, Does microstructure matter for statistical nanoindentation techniques? Cem. Concr. Compos. 32 (1) (2010) 92–99.
[9] I.G. Richardson, The nature of the hydration products in hardened cement pastes, Cem. Concr. Compos. 22 (2) (2000) 97–113.
[10] H.M. Jennings, Refinements to colloid model of C-S-H in cement: CM-II, Cem. Concr. Res. 38 (3) (2008) 275–289.
[11] P. Trtik, B. Munch, P. Lura, A critical examination of statistical nanoindentation on model materials and hardened cement pastes based on virtual experiments, Cem. Concr. Compos. 31 (10) (2009) 705–714.
[12] W. Kunther, S. Ferreiro, J. Skibsted, Influence of the Ca/Si ratio on the compressive strength of cementitious calcium-silicate-hydrate binders, J. Mater. Chem. A 5 (33) (2017) 17401–17412.
[13] M.J.A. Qomi, et al., Combinatorial molecular optimization of cement hydrates, Nat. Commun. (5) (2014).
[14] P.J.M. Monteiro, G.Q. Geng, D. Marchon, J.Q. Li, P. Alapati, K.E. Kurtis, M.J.A. Qomi, Advances in characterizing and understanding the microstructure of cementitious materials, Cem. Concr. Res. 124 (2019).
[15] G.Q. Geng, R.J. Myers, M.J.A. Qomi, P.J.M. Monteiro, Densification of the interlayer spacing governs the nanomechanical properties of calcium-silicate-hydrate, Sci. Rep. 7 (2017).
[16] G.Q. Geng, R.J. Myers, J.Q. Li, R. Maboudian, C. Carraro, D.A. Shapiro, P.J.M. Monteiro, Aluminum-induced dreierketten chain cross-links increase the mechanical properties of nanocrystalline calcium aluminosilicate hydrate, Sci. Rep. 7 (2017).
[17] F. Battocchio, P.J.M. Monteiro, H.R. Wenk, Rietveld refinement of the structures of 1.0 C-S-H and 1.5 C-S-H, Cem. Concr. Res. 42 (11) (2012) 1534–1548.
[18] G.Q. Geng, J.Q. Li, Y. Zhou, L. Liu, J.Y. Yan, M. Kunz, P.J.M. Monteiro, A high-pressure X-ray diffraction study of the crystalline phases in calcium aluminate cement paste, Cem. Concr. Res. 108 (2018) 38–45.
[19] E. L'Hopital, B. Lothenbach, D.A. Kulik, K. Scrivener, Influence of calcium to silica ratio on aluminium uptake in calcium silicate hydrate, Cem. Concr. Res. 85 (2016) 111–121.
[20] Gardner, D.W., J. Li, A. Morshedifard, S. Masoumi, M.J.A. Qomi, P. Monteiro, R. Maboudian, and C. Carraro, The nature of chemical bonds in binding phases of concrete. Energy Environ. Sci., (submitted).
[21] G.Q. Geng, J.Q. Li, Y.S. Yu, D.A. Shapiro, D.A.L. Kilcoyne, P.J.M. Monteiro, Nanometer-resolved spectroscopic study reveals the conversion mechanism of CaO center dot Al2O3 center dot 10H(2)O to 2CaO center dot Al2O3 center dot 8H(2)O and 3CaO center dot Al2O3 center dot 6H(2)O at an elevated temperature, Cryst. Growth Des. 17 (8) (2017) 4246–4253.
[22] S.K. Lee, P.J. Eng, H.K. Mao, Probing of pressure-induced bonding transitions in crystalline and amorphous earth materials: insights from X-ray Raman scattering at high pressure, Spectroscopic Methods in Mineralology and Materials Sciences, 78 2014, pp. 139–174.
[23] D.J. Dunstan, Theory of the gasket in diamond anvil high-pressure cells, Rev. Sci. Instrum. 60 (12) (1989) 3789–3795.
[24] U. Bergmann, P. Glatzel, S.P. Cramer, Bulk-sensitive XAS characterization of light elements: from X-ray Raman scattering to X-ray Raman spectroscopy, Microchem. J. 71 (2–3) (2002) 221–230.
[25] Y.M. Xiao, P. Chow, G. Boman, L.G. Bai, E. Rod, A. Bommannavar, C. Kenney-Benson, S. Sinogeikin, G.Y. Shen, New developments in high pressure X-ray spectroscopy beamline at High Pressure Collaborative Access Team, Rev. Sci. Instrum. 86 (7) (2015).
[26] J.H. Moon, J.E. Oh, M. Balonis, F.P. Glasser, S.M. Clark, P.J.M. Monteiro, Pressure induced reactions amongst calcium aluminate hydrate phases, Cem. Concr. Res. 41 (6) (2011) 571–578.
[27] J. Moon, S. Yoon, R.M. Wentzcovitch, S.M. Clark, P.J.M. Monteiro, Elastic properties of tricalcium aluminate from high-pressure experiments and first-principles calculations, J. Am. Ceram. Soc. 95 (9) (2012) 2972–2978.
[28] C.J. Sahle, et al., Formation of CaB6 in the thermal decomposition of the hydrogen storage material Ca(BH4)(2), Phys. Chem. Chem. Phys. 18 (29) (2016) 19866–19872.
[29] J.Q. Li, G.Q. Geng, R. Myers, Y.S. Yu, D. Shapiro, C. Carraro, R. Maboudian, P.J.M. Monteiro, The chemistry and structure of calcium (alumino) silicate hydrate: a study by XANES, ptychographic imaging, and wide- and small-angle scattering, Cem. Concr. Res. 115 (2019) 367–378.
[30] J.Q. Li, G.Q. Geng, W.X. Zhang, Y.S. Yu, D.A. Shapiro, P.J.M. Monteiro, The hydration of beta- and alpha(H)'-dicalcium silicates: an X-ray spectromicroscopic study, ACS Sustain. Chem. Eng. 7 (2) (2019) 2316–2326.
[31] K.P. Nagle, G.T. Seidler, E.L. Shirley, T.T. Fister, J.A. Bradley, F.C. Brown, Final-state symmetry of Na 1s core-shell excitons in NaCl and NaF, Phys. Rev. B 80 (4) (2009).
[32] C. Sternemann, M. Wilke, Spectroscopy of low and intermediate Z elements at extreme conditions: in situ studies of earth materials at pressure and temperature via X-ray Raman scattering, High Pressure Res. 36 (3) (2016) 275–292.
[33] G.Q. Geng, R.N. Vasin, J.Q. Li, M.J.A. Qomi, J.Y. Yan, H.R. Wenk, P.J.M. Monteiro, Preferred orientation of calcium aluminosilicate hydrate induced by confined compression, Cem. Concr. Res. 113 (2018) 186–196.
[34] P. Aghdasi, C.P. Ostertag, Green ultra-high performance fiber-reinforced concrete (G-UHP-FRC), Constr. Build. Mater. 190 (2018) 246–254.
[35] M. Vandamme, F.J. Ulm, Nanogranular origin of concrete creep, Proc. Natl. Acad.

Sci. U. S. A. 106 (26) (2009) 10552–10557.
[36] H. Bei, E.P. George, J.L. Hay, G.M. Pharr, Influence of indenter tip geometry on elastic deformation during nanoindentation, Phys. Rev. Lett. 95 (4) (2005).
[37] A.C. Fischer-Cripps, Elastic-plastic indentation stress fields, Introduction to Contact Mechanics, Springer US, Boston, MA, 2007, pp. 137–150.
[38] J. Ibanez, L. Artus, R. Cusco, A. Lopez, E. Menendez, M.C. Andrade, Hydration and carbonation of monoclinic C2S and C3S studied by Raman spectroscopy, J. Raman Spectrosc. 38 (1) (2007) 61–67.
[39] M. Borland, et al., The Upgrade of the Advanced Photon Source, (2018).